Input Force Estimation Using an Inverse Structural Filter

Adam D. Steltzner and Daniel C. Kammer
Department of Engineering Physics
University of Wisconsin
Madison, WI 53706

Abstract

A new method for the estimation of structural input forces is presented. The time domain technique uses a non-causal inverse structural filter (ISF) which takes as input, the structural response data, and returns, as output, an estimate the input forces. Pseudo-real-time estimation of input forces for non-collocated sensor/actuator pairs is possible for multi-input/multi-output (MIMO) systems. The formulation allows the estimation of input forces for systems that possess unstable transmission zeros and hence are non-minimum phase. Input force estimation for such systems is difficult due to the unstable nature of the non-collocated inverse system. The theory for the development of the ISF is discussed and the applicability of the formulation is derived from linear system theory. Two examples are discussed. The first is a single-input/single-output (SISO) one-dimensional spring/mass chain in which a remote accelerometer is used to estimate an input force at one end. In the second example, the technique is used to estimate six docking forces and moments between the Space Shuttle and the Russian MIR Space Station during a docking simulation.

Introduction

The estimation of dynamic forces acting on a structure is an old problem that has been treated with only partial success. Methods for such estimation fall into two categories direct methods and indirect methods. Direct methods use the placement of force transducers into the load paths at the point of force application. Indirect methods use other sensor types, placed at locations on the structure that may not necessarily correspond to the force input locations. Many situations require indirect methods because the forces cannot be measured. In general, the indirect approach to force estimation is more difficult [1] and is called an “inverse problem”. As such it is ill-posed and ill-conditioned [2]. This has made work in this area slow and the gains modest.

Currently, there are several indirect methods for identifying input forces acting on a structure [3]. The techniques are either frequency domain based or time domain based. Frequency domain techniques have been shown to have severe ill-conditioning at frequencies associated with the natural frequencies of the structure [1]. These techniques also prohibit real-time or near real-time force estimation.

Time domain techniques are more recent developments. The Sum of Weighted Accelerations Technique (SWAT) [4] has been successfully applied to a variety of different real world impact and collision problems. The limitation of this technique lies in the fact that it can only reconstruct the sum of the external forces acting on a body’s center of mass and not the individual applied forces. More recently Genaro and Rade [5] have put forth a method based on a variation of SWAT. Genaro and Rade’s method uses an integration of the accelerations to generate velocities and displacements. An inversion of the modal matrix is then used to solve the equations of motion to yield the input forces. There is also a limitation to the use of this method. The number of sensors must be equal to or greater than the number of modes responding. This can be prohibitive for a large structure with many closely spaced modes.

The focus of this paper is a new method for indirect force estimation. The proposed technique only requires as many sensors as force input locations. The method has been successful in estimating the individual input forces for structures where the sensors are not collocated with the force input locations. This is the most general of the indirect estimation cases and a problem which has to date not been successfully solved in the time domain [6, 7]. The method uses a non-causal inverse structural filter (ISF) which can be thought of as a compressed generalized pulse response for the inverse structural system. The inverse system is a state-space representation of the structure in which the input and output have been interchanged.

The proposed technique does not rely on a mathematical model of the structure, such as a FEM, but rather the ISF is identified during a standard vibration test of the structure, usually performed prior to the system being placed in service. Both force inputs and the response are measured, and the subsequently identified Markov parameters are inverted to generate the ISF. Once the system is placed in service, operational sensor data can then be fed into the ISF to generate an estimate of the input force time history. This process can be carried out in near real time to give a running estimate of the forces applied to the structure.

Background Theory

Consider a multi-degree of freedom structural system represented by the discrete-time first order state space equation

$$x_{k+1} = Ax_k + Bu_k \tag{1}$$

Here $x_k \in \Re^n$, is the state vector for the n-state system, $u_k \in \Re^{n_a}$, is the input force vector, $A \in \Re^{nxn}$, is the plant matrix and $B \in \Re^{nxn_a}$, is the input influence matrix. Using accelerometers as sensors, we can construct an output equation given by

$$y_k = Cx_k + Du_k \tag{2}$$

where $C \in \Re^{n_s x n}$, is the output influence matrix and $D \in \Re^{n_s x n_a}$, is the direct throughput matrix. We will refer to this system as having n states, n_a inputs and n_s outputs.

Assuming zero initial conditions, the system given by Eq. (1) and Eq. (2) can be stepped forward in time to write an expression for the pulse response of the forward structure

$$y_k = \sum_0^{\infty} h_i u_{k-i} \tag{3}$$

where the Markov parameters, h_i, have the form

$$h_0 = D, h_i = CA^{i-1}B, i = 1, 2, ... \tag{4}$$

This is a multi-input/multi-output (MIMO) moving average representation of the input/output relationship for the forward structural system with $h_i \in \Re^{n_s x n_a}$. It can be shown [8] that there are only $2n_{oc}+1$ independent Markov parameters, where n_{oc} is the number of observable and controllable modes of the system. If an auto-regressive moving average representation is used, the result is an observer Markov parameter formulation of the pulse response [8]. This formulation only requires $2n_{oc}+1$ observer Markov parameters to be a complete representation of the forward structure.

Equations (1) and (2) can be manipulated to interchange the input and output, yielding the inverse structural system equations [9] in the form

$$\begin{aligned} x_{k+1} &= \hat{A}x_k + \hat{B}y_k \\ u_k &= \hat{C}x_k + \hat{D}y_k \end{aligned} \tag{5}$$

in which the inverse system plant, input influence, output influence, and direct throughput matrices defined as

$$\begin{aligned} &\hat{A} = [A - BD^+C], \qquad \hat{B} = BD^+ \\ &\hat{C} = -D^+C, \qquad\qquad \hat{D} = D^+ \\ &D^+ = (D^T D)^{-1} D^T \end{aligned} \tag{6}$$

The Moore-Penrose pseudo-inverse, D^+, requires that the number of sensors, n_s, be greater than the number of force inputs, n_a, for a unique inverse system to exist. Further, D must be full column rank for D^+ to exist. Note that the inverse plant matrix, $\hat{A}$, can be unstable. For structural systems with sensors at different locations than the force input locations, called non-collocated structures, the forward system possesses non-minimum phase zeros. It can be shown that these zeros, which have positive real parts, are eigenvalues of the inverse system. This creates an unstable inverse system.

As with the forward system, a pulse response sequence can be written for a stable inverse system. Based on the assumption of zero initial conditions

$$u_k = \sum_0^{k} \hat{h}_i y_{k-i} \tag{7}$$

where the inverse system Markov parameters are given by

$$\hat{h}_0 = \hat{D}, \ \ \hat{h}_i = \hat{C}\hat{A}^{i-1}\hat{B}, \ \ i = 1, 2, ... \tag{8}$$

This is a MIMO moving average representation of the input/output relationship for the inverse structural system with $\hat{h}_i \in \Re^{n_a x n_s}$. As mentioned above, the relationship given in Eq. (7) is not always a converging sum. Furthermore, even for systems in which Eq. (7) is a well behaved stable relationship, the calculation of the inverse system Markov parameters via Eq. (8), or some simple recursive relationship based on Eq. (3), has been shown to be numerically unstable due to the intrinsic ill-conditioning found in the inverse problem [6].

For real-time or near real-time force estimation, a relationship similar to that found in Eq. (7) is desired. It can be shown that, for non-minimum phase structural systems, D drops rank and the Moore-Penrose pseudo-inverse in Eq. (6) does not exist. In such cases, the causal expression in Eq.(7) cannot be written. Consider a system in which all the sensors and force inputs are non-collocated. For such a system, under the assumption of non-minimum phase, the direct throughput matrix is the zero matrix, producing

$$\begin{aligned} x_{k+1} &= Ax_k + Bu_k \\ y_k &= Cx_k \end{aligned} \tag{9}$$

This system must be stepped forward in time before inversion can take place. The new forward system is

$$\begin{aligned} x_{k+1} &= Ax_k + Bu_k \\ y_{k+1} &= CAx_k + CBu_k \end{aligned} \tag{10}$$

The inverse system associated with Eq (10) is non-causal. That is, the estimate of the input force at time k is now a function of the response at future times, k+1 through k+l. In general, if the first l-1 Markov parameters in Eq.(4) are zero, that is $D=CB=CAB=\ldots=CA^{l-2}B=0$, then we can construct the non-causal, general "l-lead" inverse model in the form

$$u_k = \sum_{i=0}^{k} \hat{h}_i y_{k+l-i} \quad (11)$$

where again

$$\hat{h}_0 = \hat{D},\ \ \hat{h}_i = \hat{C}\hat{A}^{i-1}\hat{B} \quad i = 1,2,3..., \quad (12)$$

and now

$$\begin{aligned} \hat{A} &= [A - B(CA^{l-1}B)^{+}(CA^{l})], \quad \hat{B} = B(CA^{l-1}B)^{+} \\ \hat{C} &= -(CA^{l-1}B)^{+}(CA^{l}), \quad \hat{D} = (CA^{l-1}B)^{+} \end{aligned} \quad (13)$$

If an l-lead inverse is constructed for a forward system which has some collocated sensor/force input pairs and some non-collocated sensor/force input pairs, then the l-lead inverse ignores the contribution of the first l-1 Markov parameters to the pulse response.

For real-time or near real-time force estimation, a relationship similar to that found in Eqs. (7) or (11) is desired. In general, Eqs. (7) and (11) have an unbounded number of terms. A finite non-causal MA model of the inverse structure must be generated for force estimation.

Inverse Structural Filter Formulation

It has been found that a finite length, non-causal filter, can be used to treat difficult non-minimum phase, non-collocated, structural systems that have previously not been amenable to force estimation. The ISF has the form

$$u_k = \sum_{i=0}^{N_R-1} r_i y_{k-i+l} \quad (14)$$

or

$$\begin{aligned} u_k &= r_0 y_{k+l} + r_1 y_{k+l-1} + \cdots + r_l y_k + r_{l+1} y_{k-1} + \cdots \\ &+ r_{N_R-2} y_{k+l-N_R+2} + r_{N_R-1} y_{k+l-N_R+1} \end{aligned}$$

where l is the non-causal lead, r_i is the ith ISF weight and N_R is the ISF size. For multi-input/multi-output (MIMO) systems, we note that r_i is a matrix with $r_i \in \Re^{n_a x n_s}$. These weights are a set of pseudo inverse system Markov parameters. Finding the values of the weights amounts to solving a deconvolution problem.

A common approach to solving the deconvolution problem is to cast it in terms of a matrix inversion problem. We can assemble the ISF weights with $R = [r_0 \quad r_1 \quad \cdots \quad r_{N_R-1}]$, where $R \in \Re^{n_a x (N_R n_s)}$. The convolution relationship between the input and output data can then be formed as the matrix inversion problem given by

$$RY = U \quad (15)$$

with

$$R = UY^{+} \quad (16)$$

Here we have defined, Y and U to be the following

$$Y = \begin{bmatrix} \tilde{y}_0 & \tilde{y}_1 & \cdots & \cdots & \tilde{y}_{Nc-1} \\ 0 & \tilde{y}_0 & \cdots & \cdots & \tilde{y}_{Nc-2} \\ 0 & 0 & \cdots & \cdots & \tilde{y}_{Nc-3} \\ \vdots & \vdots & \ddots & \cdots & \vdots \\ 0 & 0 & \tilde{y}_0 & \cdots & \tilde{y}_{Nc-Nr} \end{bmatrix} \quad (17)$$

$$U = \Big[\underbrace{0 \ \ \cdots \ \ 0}_{l} \quad \tilde{u}_0 \quad \tilde{u}_1 \quad \cdots \quad \tilde{u}_{N_R-l-1}\Big] \quad (18)$$

The entries in U have been shifted by l blocks to generate the non-causal lead for the model, as reflected in Eq. (14). The "~" in the definitions for Y and U represent ensembles from different experiments used to build the rank of Y, giving

$$\begin{aligned} \tilde{y}_i &= [y_i^1 \quad y_i^2 \quad y_i^3 \quad \cdots \quad y_i^{n_{\exp}}],\ \tilde{y}_i \in \Re^{n_s x n_{\exp}},\ y_i^k \in \Re^{n_s x 1} \\ \tilde{u}_i &= [u_i^1 \quad u_i^2 \quad u_i^3 \quad \cdots \quad u_i^{n_{\exp}}],\ \tilde{u}_i \in \Re^{n_a x n_{\exp}},\ u_i^k \in \Re^{n_a x 1} \end{aligned} \quad (19)$$

Inspection of Eq. (15) indicates that there are $n_a*(N_R n_s)$ unknowns and $(n_a N_R)*n_{exp}$ equations. This suggests that the number of experiments must be at least as great as the number of inputs in order to obtain a unique solution. Even when this is the case the solution may not be unique. The row rank of Y depends on the input characteristics as well as the number of observable and controllable modes in the system. In practice, the matrix Y is frequently rank deficient. The pseudo-inverse of row rank deficient Y is calculated by a truncated singular value decomposition (TSVD) method [10] and the resulting ISF is the minimum norm solution. This solution is only unique with respect to the row space of the data matrix Y.

Although Eq. (14) is a straightforward representation of the ISF, the form in Eq. (16) is not numerically conducive to the calculation of the ISF weights given in R. It has been observed through experience, that better results are obtained by using an alternate formulation of the ISF deconvolution problem. We begin the formulation of this alternate approach with the known result that the convolution of the forward pulse response and the inverse system pulse response generates the unit pulse. That is, for a discrete time sequence of length n_t, we have

$$c_k = \sum_{i=0}^{k} h_i \hat{h}_{k-i}$$
$$c = \begin{bmatrix} c_0 & c_1 & \cdots & c_{nt-1} \end{bmatrix} = \begin{bmatrix} I & 0 & \cdots & 0 \end{bmatrix} \quad (20)$$

This can be enforced for the finite length ISF using the relationship

$$RH = \begin{bmatrix} I & 0 & \cdots & 0 \end{bmatrix} \quad (21)$$

where R is defined as before and

$$H = \begin{bmatrix} h_0 & h_1 & h_2 & \cdots & h_{N_R-1} & \cdots & h_{Nc-1} \\ 0 & h_0 & h_1 & \cdots & h_{N_R-2} & \cdots & h_{Nc-2} \\ 0 & 0 & h_0 & \cdots & h_{N_R-3} & \cdots & h_{Nc-3} \\ \vdots & \vdots & \vdots & \ddots & \vdots & \vdots & \vdots \\ 0 & 0 & 0 & \cdots & h_0 & \cdots & h_{Nc-Nr} \end{bmatrix} \quad (22)$$

in which, $H \in \Re^{(n_s N_R) x (n_a N_C)}$. In theory, for perfect noise free Markov parameters, it can be shown that the relationship $N_R(n_s - n_a) \le 2 n_{oc} n_a$ insures that the data matrix H is full row rank. In practice, with noise corrupted data, it is quite often the case that the rank building of H happens very slowly and H is often not full row rank. In this case the pseudo-inverse of H is calculated by a TSVD method and the resulting ISF is the minimum norm solution.

To generate the non-causal ISF, the pulse in Eq. (21) is modified by a l-length lag, producing

$$RH = [\underbrace{0 \;\; \cdots \;\; 0}_{l} \;\; I \;\; \underbrace{0 \;\; \cdots \;\; 0}_{n_t - l - 1}] \quad (23)$$

This yields the ISF model given by

$$R = [0 \;\; \cdots \;\; 0 \;\; I \;\; 0 \;\; \cdots \;\; 0] H^+ \quad (24)$$

This method of computation is superior because the forward Markov parameters that make up H are usually calculated from the averaging of several vibration test records. This averaging reduces the effects of error in the sensor data. Note, that H is inverted only once in the calculation of the ISF regardless of the non-causal lead. This means that a large set of non-causal leads can be investigated at a low computational cost. It is worth noting that Eq. (16) and Eq. (24) return the same ISF only if the respective data matrices, Y and H are full row rank. In this case the pseudo-inverse is the Moore-Penrose pseudo-inverse. If Y and H are not full row rank, then the ISFs produced by each method are the minimum norm solutions based on the range of the row space of the data matrices Y and H. These row spaces are, in general, different, so the resulting ISFs are different, although the force estimates produced by each ISF are almost identical.

Examples

<u>1-D Spring-Mass Chain</u>

The first example is that of a simple one-dimensional spring and mass chain shown in Figure 1. This model has ten DOF and has been given 2.0% modal damping.

The input force is applied at the left end of the chain and the acceleration response is measured at DOF #8 near the right end. The structure has one rigid body mode and nine elastic modes from 22-140 Hz.

A virtual vibration test was conducted for this structure using MATLAB and the forward pulse response sequence, or Markov parameters, were obtained. During the vibration test, the sensor response was corrupted by the addition of white noise with an amplitude of 10.0% of the RMS sensors response using

$$y_{noisy} = y + 0.10\left(\frac{\sqrt{\sum y_i^2}}{n_t}\right)\eta \quad (25)$$

Here n_t is the number of data points used in the test, y is an n_t length vector of the response, y_{noisy} is the noise corrupted version of y and η is an n_t length vector of normally distributed random numbers with variance equal to 1. The Markov parameters are then used to identify several ISF's each with a different non-causal lead. The ISF's can be used to generate force estimations for a broadband input and the ISF with the best accuracy is then chosen. This is an empirical method for finding the optimal non-causal lead.

For this example, a 100 tap ISF was generated and 16 different non-causal leads were investigated ranging from l=0 to l=95. The most accurate model was that with l=30. The identified ISF's were then applied to the estimation of an arbitrary input force consisting of a random combination of ten sinusoids ranging in frequency from 0-140 Hz. Again the response data used to build the input force estimation was corrupted as above with 10.0% RMS white noise. In Figures 2 and 3, we see the results of an estimation of the sample input in the time and frequency domains, respectively. The force estimate has been lowpass filtered with a break frequency of 140 Hz.

In Figure 3, an unfiltered version of the force estimate has also been included. This is shown to indicate the problems associated with estimating forces outside the frequency range of the structural response. The highest natural frequency for this structure is 141.0 Hz. Above this frequency, noise starts to dominate and force estimates become very unreliable. It is instructive to plot the percent RMS error of these force estimates for different non-causal leads using the relationship

$$\varepsilon_{\%RMS} = 100\%(\frac{\sqrt{\sum (u_{est_i} - u_{act_i})^2}}{\sqrt{\sum u_{act_i}^2}}) \qquad (26)$$

where u_{act_i} and u_{est_i} are the actual and estimated forces. Figure 4 demonstrates the improved estimates with different non-causal leads and displays the effect of noise corruption of the sensor response data used in the force estimation. Such a non-causal lead comparison resulted in the choice of l=30 for the reported force estimates.

As indicated above, this method is successful in the estimation of non-collocated forces, using rather small models. The above ISF possessed just 100 terms. It is worth noting that this method can also be used to estimate collocated or drive-point force time histories. The results are comparable, with errors in the estimates being slightly higher (25% RMS for this example).

Shuttle/MIR

The second application of this method is the estimation of docking forces between the Space Shuttle and the Russian MIR space station using numerically simulated response data. As part of the NASA/JSC sponsored program for assessing the structural health of the MIR, a FEM of the MIR structure was used to generate vibration test data and force estimation data. The Russian built FEM contains 2646 DOF and has 211 modes under 5.0 Hz. The mass and stiffness matrices from this model were used to construct a state-space representation of the structural system using 25 sensor DOFs and 6 input DOFs. All modes were assumed to possess 2% critical damping. A plot of the FEM with the sensor DOFs indicated is shown in Figure 5.

There are 25 accelerometers on the MIR of which 13 were used to estimate the docking forces. In this example, the proposed method will be used to estimate a set of known input forces and moments applied to the docking node in the FEM. The known input forces and moments come from Lockheed Martin Corporation's estimates of the docking forces for STS-81. These estimates were based on kinematical data taken just prior to the docking event and used as the basis for a non-linear direct transient finite element analysis.

A state-space representation of the MIR possessing the 6 docking input DOFs and the chosen 13 sensor DOFs was used to perform a virtual vibration test to identify the forward Markov parameters. During this test, each channel of the sensor response was corrupted with noise as per Eq. (25). Forty averages of the vibration test data were used to generate the Markov parameters. The Markov parameters were then used to compute the ISF, with several non-causal leads evaluated. The best model lead was found to be l=30. A typical ISF (sensor DOF 104014-y and z-direction input force) is plotted in Figure 6.

The three known force time histories and three known moment time histories were then applied to the 6 DOFs corresponding to the docking location and the response was simulated numerically. Again, each channel of the response data from the accelerometer locations was corrupted with white noise as above. A comparison of the known input forces and the estimates from the noise corrupted response data is shown in Figure 7. These estimates have been lowpass filtered with a break frequency of 5.5 Hz. Figure 8 shows an enlargement of a portion of Figure 7. Inspection indicates that the estimates are very accurate. The fraction RMS errors for the above x, y and z components of the input forces were, 22%, 57% and 9.5% respectively. It should be noted that such an estimate of error is not appropriate for transient forces. The estimated forces persist at a low level after the actual forces decay, and this discrepancy drives the apparent %RMS error up. The estimated input moments are not as accurate. Figure 9 shows the estimates for the input moments in the x, y and z directions. Again these estimates have been lowpass filtered with a break frequency of 5.5 Hz.

As a final check of the quality of the force and moment estimates, they are re-applied to the forward system and the resulting response is compared with the actual response. Figure 10 shows a comparison for a typical response channel (104014-z). The relatively close match between actual response and the response due to the estimated forces and moments suggests that the moments may not influence the response data significantly. In this case the ISF would have difficulty correctly estimating the input moments. In general, if there is little information present in the response time series regarding the input forces, use of that response for force reconstruction will fail. Future work will focus on quantifying the forward system requirements for ISF input force estimation success.

Conclusion

A novel method for force estimation has been presented. This method, which uses a vibration-test-identified, non-causal moving average filter to represent the inverse structural system, has been shown to be successful in estimating input forces in structural systems in which the response sensors are non-collocated with the force input locations. These non-minimum phase problems have typically been beyond the capability of currently used techniques. It has been observed that the method can be unsuccessful in certain instances and future work will focus on the identifying which features of the forward structural system lead to these observed difficulties.

Acknowledgments

The above work was conducted with support from NASA Johnson Space Flight Center under Grant NAG9-953. The authors wish to thank Rocket and Space Corporation-Energia (RSC-E) for the MIR FEM, Lockheed Martin Corporation for the STS-81 docking load predictions, and Mr. James Dagen at NASA/JSC for his support and encouragement. The authors would additionally like to thank Professor Paul Milenkovic at U.W. Madison for his continued support and guidance.

References

1. Starkey, J.M. and G.L. Merrill, *On the Ill-Conditioned Nature of Indirect Force-Measurement Techniques.* Journal of Modal Analysis, 1989. (7): p. 103-108.

2. Groetsch, C.W., *Inverse Problems in the Mathematical Sciences*. 1993, Braunschweig: Vieweg. 152.

3. Stevens, K.K. *Force Identification Problems- An Overview*. in *SEM Spring Conference on Experimental Mechanics*. 1987. Houston, Texas: SEM.

4. Carne, T.G., V.I. Bateman, and R.L. Mayes. *Force Reconstruction Using a Sum of Weighted Accelerations Technique*. in *10th International Modal Analysis Conference*. 1992. San Diego, Ca.: SEM.

5. Genaro, G. and D.A. Rade. *Input Force Identification in the Time Domain*. in *16th International Modal Analysis Conference*. 1998. Santa Barbara, California: SEM.

6. Kammer, D.C. *Input Force Reconstruction Using a Time Domain Technique*. in *AIAA Dynamic Specialist Conference*. 1996. Salt Lake City, Utah: AIAA.

7. Horta, L.G. and C.A. Sandridge. *On-Line Identification of Forward/Inverse Systems for Adaptive Control Applications*. in *Proceedings of the 1992 Guidance, Navigation and Control Conference.* 1992. AIAA.

8. Juang, J.-N., *Applied System Identification*. 1 ed. 1994, Englewood Cliffs, New Jersey 07632: Prentice Hall PTR. 394.

9. Kammer, D.C., *Estimation of Structural Response Using Remote Sensor Locations.* Journal of Guidance, Control and Dynamics, 1997. 20(3): p. 501-508.

10. Golub, G.H. and C.F.V. Loan, *Matrix Computations*. 2 ed. 1989, Baltimore: The Johns Hopkins University Press. 642.

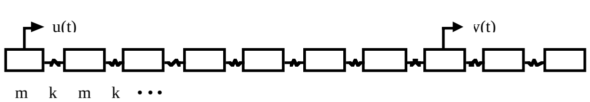

Fig. 1. One Dimensional Spring Mass Chain.

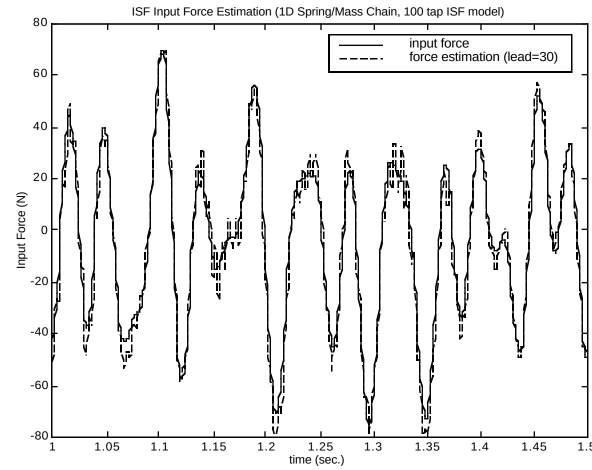

Fig. 2. Actual and Estimated Input Forces, 15.6% RMS error.

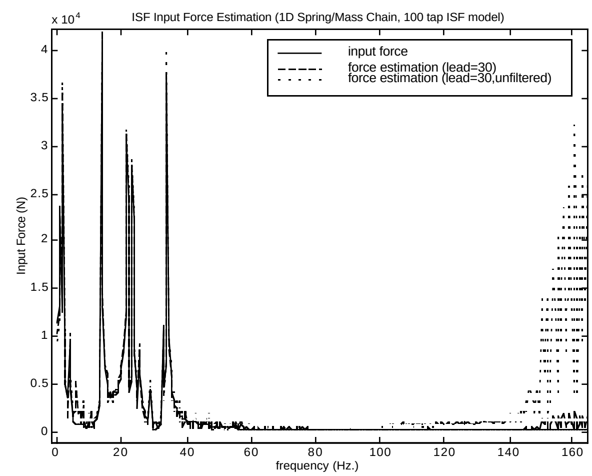

Fig. 3. Actual and Estimated Input Forces, 15.6% RMS error (filtered), 350+% RMS error (unfiltered).

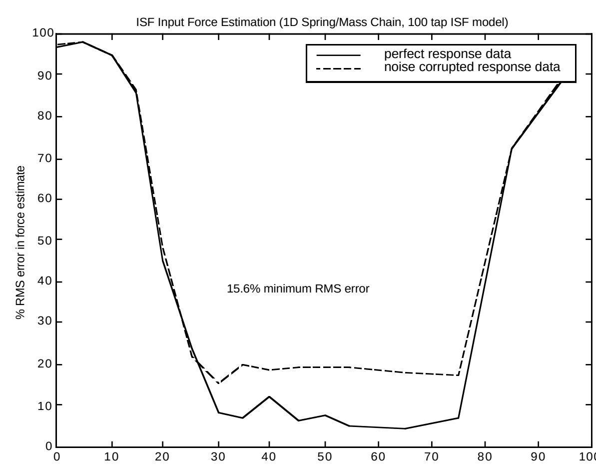

Fig. 4. % RMS Error in Force Estimates with Model Lead.

Fig. 5. MIR FEM with Sensor Locations Shown.

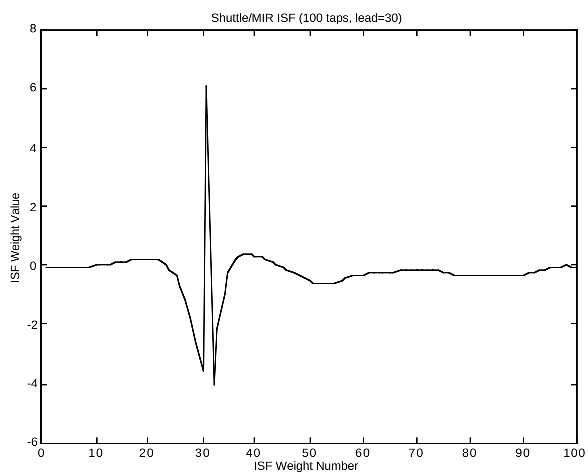

Fig. 6. Typical ISF (104014-y to z-direction input force).

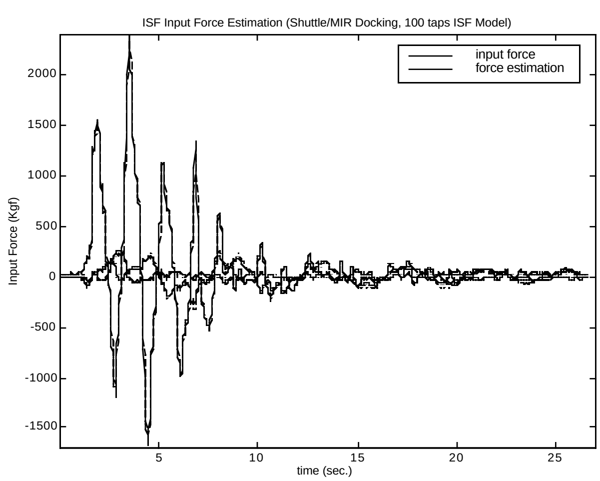

Fig. 7. Shuttle/MIR Docking Simulation Force Estimates.

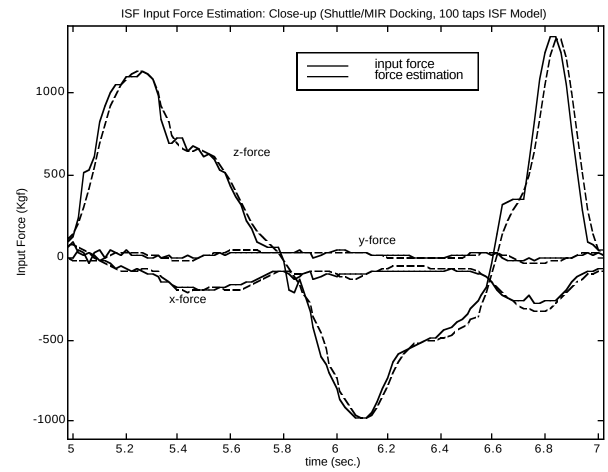

Fig. 8. Shuttle/MIR Docking Simulation Force Estimates.

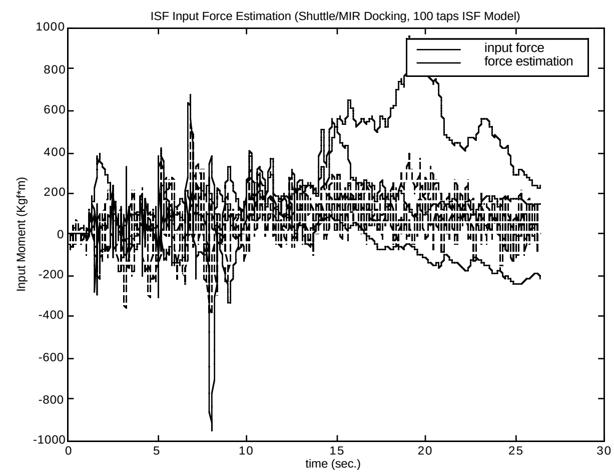

Fig. 9. Shuttle/MIR Docking Simulation Moment Estimates.

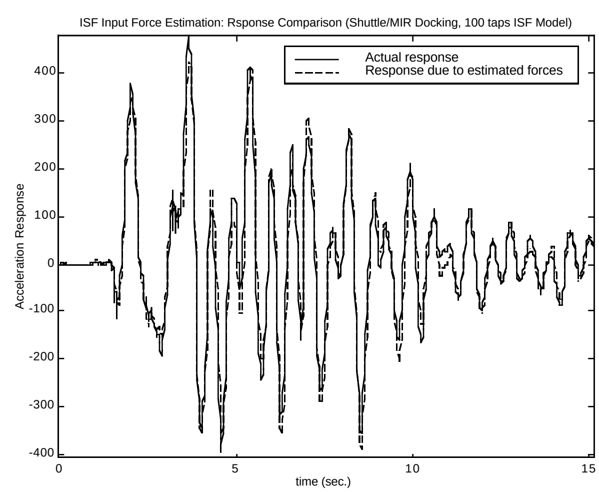

Fig. 10. Shuttle/MIR Docking Simulation Response Comparison (sensor DOF 104014-z).